

FULL PAPER

Biological evaluation of selected 3,4-dihydro-2(1H)-quinoxalinones and 3,4-dihydro-1,4-benzoxazin-2-ones: Molecular docking study

Jelena Petronijević¹ | Nenad Janković¹  | Tatjana P. Stanojković² |
Nenad Joksimović¹ | Nađa Đ. Grozdanić² | Milan Vraneš³ | Aleksandar Tot³ |
Zorica Bugarčić¹

¹ Department of Chemistry, University of Kragujevac, Kragujevac, Serbia

² Institute for Oncology and Radiology of Serbia, Belgrade, Serbia

³ Department of Chemistry, Biochemistry and Environmental Protection, University of Novi Sad, Novi Sad, Serbia

Correspondence

Dr. Nenad Janković and Prof. Zorica Bugarčić, Department of Chemistry, University of Kragujevac, Radoja Domanovića 12, 34000 Kragujevac, Serbia.
Email: nenad.jankovic@kg.ac.rs (NJ); zoricab@kg.ac.rs (ZB)

Funding information

Ministry of Education, Science and Technological Development of the Republic of Serbia, Grant numbers: 172011, 175011

Abstract

In order to investigate new potential therapeutically active agents, we investigated the biological properties of two small libraries of quinoxalinones and 1,4-benzoxazin-2-ones. The results obtained showed that compounds **5**, **9–11** have good cytotoxic activity against HeLa cells where the lowest IC₅₀ value (10.46 ± 0.82 μM/mL) was measured for compound **10**. Additionally, the most active compounds (**5**, **9–11**) showed much better selectivity for MRC-5 cells (up to 17.4) compared to cisplatin. *In vitro* evaluation of the inhibition of the enzyme α-glucosidase showed that compounds **10** and **11** exert significant inhibition of the enzyme at 52.54 ± 0.09 and 40.09 ± 0.49 μM, respectively. Competitive experiments with ethidium bromide (EB) indicated that all tested compounds have affinity to displace EB from the EB-DNA complex through intercalation, suggesting good competition with EB ($K_{sv} = (3.1 ± 0.2), (5.1 ± 0.1), (5.6 ± 0.2), \text{ and } (6.3 ± 0.2) × 10^3 \text{ M}^{-1}$). A molecular docking study was also performed to better understand the binding modes and to conclude the structure–activity relationships of the synthesized compounds.

KEYWORDS

anticancer, antidiabetic, benzoxazines, DNA and BSA interaction, quinoxalinones

1 | INTRODUCTION

Heterocycles such as quinoxalines^[1,2] and benzoxazines^[3] are structural motifs of wide spectrum of biologically active compounds. Quinoxalines display a broad spectrum of pharmacological activity such as antimicrobial,^[4] anti-inflammatory,^[5] antidiabetic,^[6] antiviral,^[7] anticancer,^[8,9] and antituberculosis.^[10] In fact, one of the primary targets in medicinal chemistry and one of the biggest health problem in society nowadays is cancer. Since cisplatin was involved in clinical practice, platinum-based drugs had been in center of researches as

chemotherapy agents.^[11,12] Use of cisplatin in clinical therapy is limited by several side effects such as neurotoxicity, nephrotoxicity,^[13–15] limited applicability, etc. Development and synthesis of new non-platinum drugs with less side effects is the major interest in medicinal chemistry.^[16] Bearing in mind these facts, we developed synthesis of novel 3,4-dihydro-2(1H)-quinoxalinones (**1–12**) and 3,4-dihydro-1,4-benzoxazin-2-ones (**13–20**) (Figure 1) as potential drugs for cisplatin replacement.^[17] The new synthesized quinoxalinones and oxazines were exposed to antitumor, anti-α-glucosidase and antiangiogenic activities, DNA and BSA binding, and docking study. Investigation of

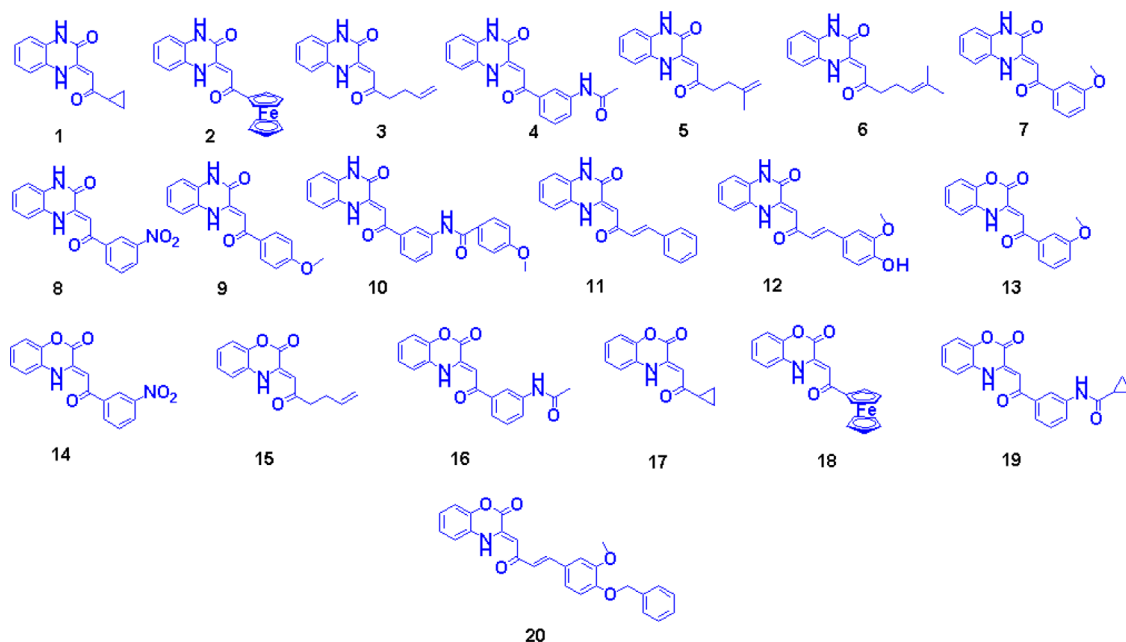


FIGURE 1 Structures of tested compounds 3,4-dihydro-2(1H)-quinoxalinones (1–12) and 3,4-dihydro-1,4-benzoxazin-2-ones (13–20)

the interaction between small molecules and DNA can be useful for creating new cancer therapy treatments or anticarcinogens^[18] or to understand the toxic properties and mechanism of harmful chemicals. Drugs and bioactive small molecules bind reversibly to albumin^[19] that plays a key role in the transportation and deposition of many biologically active compounds.^[20] Interactions between selected compounds (5, 9–11) and DNA or bovine serum albumin (BSA) were studied at normal physiological conditions using fluorescence spectral techniques.^[21] Also, the molecular docking study with DNA and BSA was performed to support the interactions and to determine the possible binding modes and binding sites.

Angiogenesis is a complex physiological process crucial for pathogenesis, in all stages of cancer progression.^[22–24] In the earlier studies, antiangiogenesis has been described as crucial strategy for tumor growth inhibition and metastasis.^[25,26] The development of new blood vessels is essential for adequate blood supply in malignancy expansion. Therefore, angiogenesis suppression is a promising approach in current anti-cancer therapy.

2 | RESULTS AND DISCUSSION

2.1 | Anticancer activity

We investigated *in vitro* the cytotoxic activity of the novel previously synthesized compounds 1–20^[17] against human cervix adenocarcinoma (HeLa), human colon carcinoma (LS174), non-small cell lung carcinoma (A549), and normal human fetal lung fibroblast cell line (MRC-5). Cisplatin was used as a reference control compound. Their cytotoxicities are shown as IC₅₀ values in Table 1. The evaluation was conducted in accordance with the Protocol of the American Cancer Institute (NCI).^[27]

It is evident that a few compounds from this series showed a good cytotoxic activity, while the other compounds have moderate to weak effects. Compounds 5, 9–11 showed a significant cytotoxic activity against all tested malignant cell lines. Likewise, we note a group of several investigated substances (1, 12, 15, and 18) that possesses moderate activity (Table 1). Also, the safety index (SI) of selected compounds was calculated versus normal MRC-5 cells (Table 2). As can be seen, compounds 5, 9–11 possess better selectivity compared to cisplatin, specially 10, where SI is 17.44 for HeLa cells. Based on achieved results, we investigated mechanism of action of four compounds that showed best anticancer activity.

The InChI codes of the investigated compounds together with some antitumor activity data are provided as Supporting Information.

2.2 | Assessment of the cell cycle distribution

Results of cell cycle distribution on HeLa cells treated with compounds 5, 9–11 for 24 h are shown on Figure 2. These compounds exhibited good cytotoxicity and inhibition of all type of investigated cell line. Based on previous we chose to examine their mechanism of action by cytofluorimetric analysis using propidium iodide to label DNA. After 24 h incubation with the investigated compounds, a slight increase in sub-G1 population was observed. However, certain dose-dependent changes in the sub-G1 distribution of HeLa cells were recorded. Regardless of the indicated good cytotoxic effect, there were any relevant change and the basal level in the G1, S, and G2-M population. Additionally, compound 11 showed better effects, leading to a notable increase in G2/M phase in HeLa cells treated with both concentrations of the compound, which was coupled with a decrease in the percentage of cells in G1 phase (Figure 2). The obtained results suggest that these compounds probably have a different mode of action.

TABLE 1 Concentrations of compounds 1–20 that induced a 50% decrease in HeLa, LS174, A549, and MRC-5 cell survival rate (expressed as $IC_{50} \pm SD$ ($\mu M/mL$))

Compound	IC_{50} ($\mu M/mL$)			
	HeLa	LS174	A549	MRC-5
1	68.90 ± 1.72	72.55 ± 1.63	96.85 ± 2.33	>200
2	>200	171.55 ± 4.26	188.11 ± 3.72	>200
3	169.61 ± 2.03	121.17 ± 1.92	95.26 ± 0.34	>200
4	23.38 ± 0.51	49.57 ± 1.22	154.33 ± 2.95	>200
5	25.12 ± 1.47	33.52 ± 1.66	86.21 ± 2.48	173.81 ± 2.88
6	93.91 ± 2.22	107.45 ± 1.48	109.70 ± 0.64	196.45 ± 4.28
7	89.98 ± 0.43	111.52 ± 3.56	125.60 ± 2.09	>200
8	>200	176.23 ± 2.57	198.01 ± 1.86	>200
9	15.19 ± 0.47	24.31 ± 1.43	66.92 ± 1.73	190.32 ± 4.79
10	10.46 ± 0.82	16.77 ± 0.31	40.41 ± 1.32	182.43 ± 3.46
11	16.57 ± 0.48	19.11 ± 1.23	22.57 ± 0.76	174.22 ± 3.55
12	60.71 ± 2.96	63.48 ± 0.45	59.66 ± 1.15	>200
13	147.61 ± 3.58	151.66 ± 2.46	153.55 ± 4.71	>200
14	172.07 ± 3.69	141.22 ± 3.58	>200	>200
15	89.88 ± 1.56	91.43 ± 0.32	96.05 ± 0.51	>200
16	161.78 ± 3.35	153.48 ± 1.05	144.44 ± 2.83	>200
17	175.32 ± 1.32	164.39 ± 1.71	>200	>200
18	70.53 ± 2.47	55.49 ± 1.26	36.59 ± 0.45	181.22 ± 1.71
19	>200	184.53 ± 1.39	191.58 ± 3.67	>200
20	68.35 ± 1.41	94.67 ± 2.79	177.52 ± 2.74	>200
Cisplatin	2.37 ± 0.28	4.83 ± 0.35	11.59 ± 1.64	14.32 ± 1.28

The compounds were incubated with cells for 72 h. IC_{50} values are expressed as the mean \pm SD (standard deviation) determined from the results of MTT assay in two independent experiments.

2.3 | Fluorescence quenching studies

2.3.1 | Fluorescence quenching on EB-DNA

In order to investigate the interaction of the compounds with DNA, the competitive binding experiment was realized. EB has low fluorescence intensity but it can be enhanced in the presence of DNA. A complex's competitive binding to EB-bound DNA can reduce the intensity due to shifting of bound EB from DNA.^[28] The fluorescence quenching spectra of titration EB-DNA with 5, 9–11 solutions were recorded in

the range of 550–750 nm (Figure 3). The fluorescence emission intensity at 610 nm of the EB-DNA solution showed a significant decrease (hypochromism) by increasing of concentrations of 5, 9–11. The observed quenching of *in situ* formed complex of EB-DNA species indicates a competition between the quenchers 5, 9–11 and EB for binding to DNA.

The fluorescence quenching of 5, 9–11 was described by means of the Stern–Volmer equation (Equation 1),^[29] implying that the dependence of I_0/I on $[Q]$ was examined

$$I_0/I = 1 + k_q \tau_0 [Q] = 1 + K_{sv} [Q] \quad (1)$$

TABLE 2 Safety index

Compounds	IC_{50} (MRC-5)/ IC_{50} (cell line)		
	HeLa	LS174	A549
5	6.92	5.18	2.01
9	12.53	7.83	2.84
10	17.44	10.88	4.51
11	10.51	9.12	7.72
Cisplatin	6.04	2.96	1.24

In Equation 1, I_0 and I are the emission intensities in the absence and presence of the quenchers, respectively, $[Q]$ is the total concentration of the quenchers, k_q is the bimolecular quenching rate constant, and τ_0 is the average lifetime of DNA in the absence of a quencher (10^{-8} s). K_{sv} is the Stern–Volmer quenching constant whose values were obtained from the slopes of the plots of I_0/I versus $[Q]$. In Table 3 are presented quenching parameters for 5, 9–11 [$(6.3 \pm 0.2) \times 10^3$, $(5.6 \pm 0.2) \times 10^3$, $(3.1 \pm 0.2) \times 10^3$, and $(5.1 \pm 0.1) \times 10^3 M^{-1}$, respectively] and these values indicate that the tested compounds have affinity

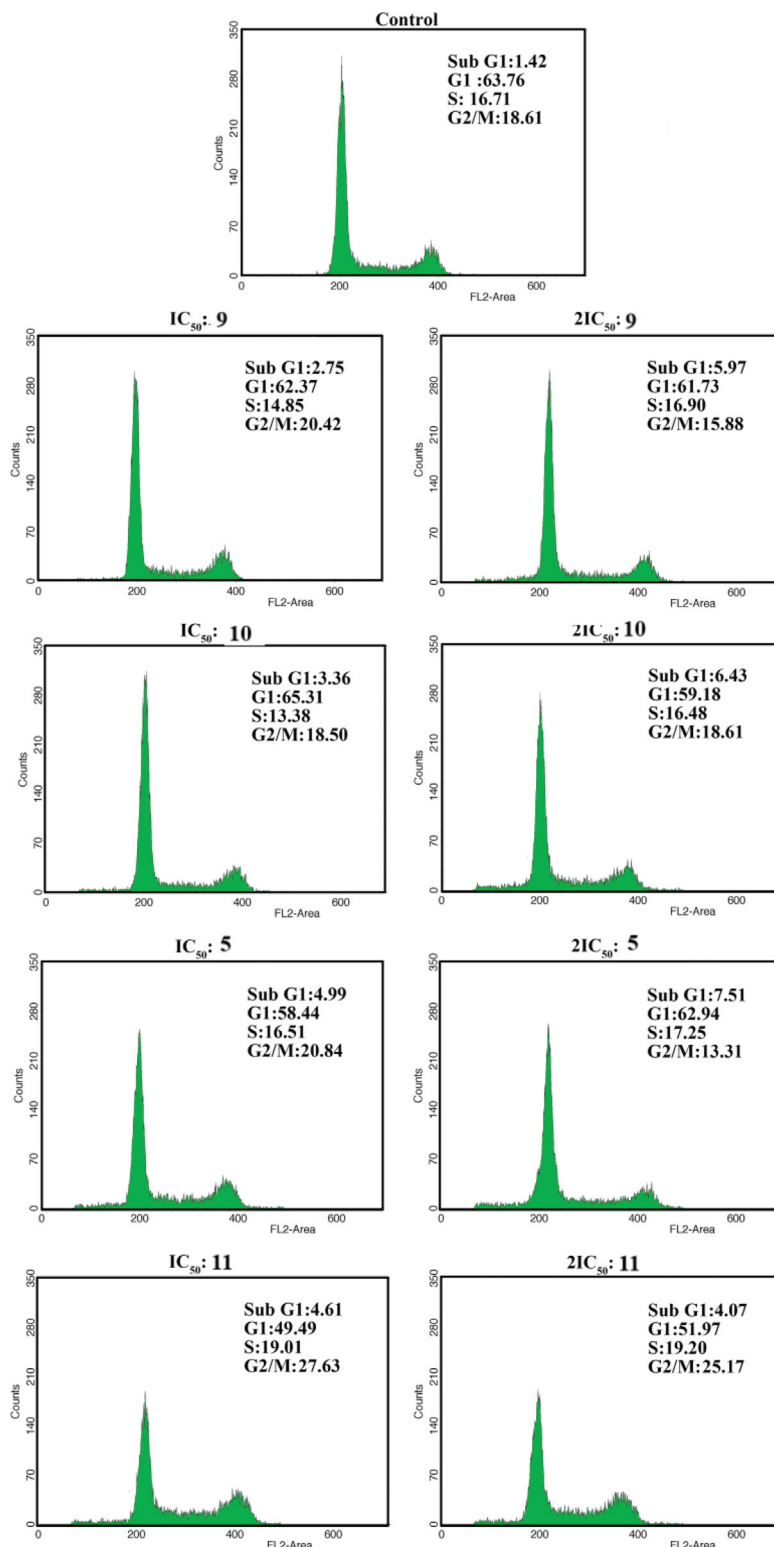


FIGURE 2 PI-flow cytometric analysis of cell cycle. Histograms present cell cycle distribution in untreated cells (control) and cells treated with 5, 9–11

to substitute EB from the EB-DNA complex and bind strongly with DNA through intercalation. Also, measured K_{sv} clearly indicated that these values are in order with the constants obtained for potential metal-drugs.^[30,31]

2.3.2 | Protein binding experiments

Bearing in mind that the efficiency of drugs strongly depends on their ability to bind to protein, we decided to investigate the affinity of compounds 5, 9–11 to bind to bovine serum albumin

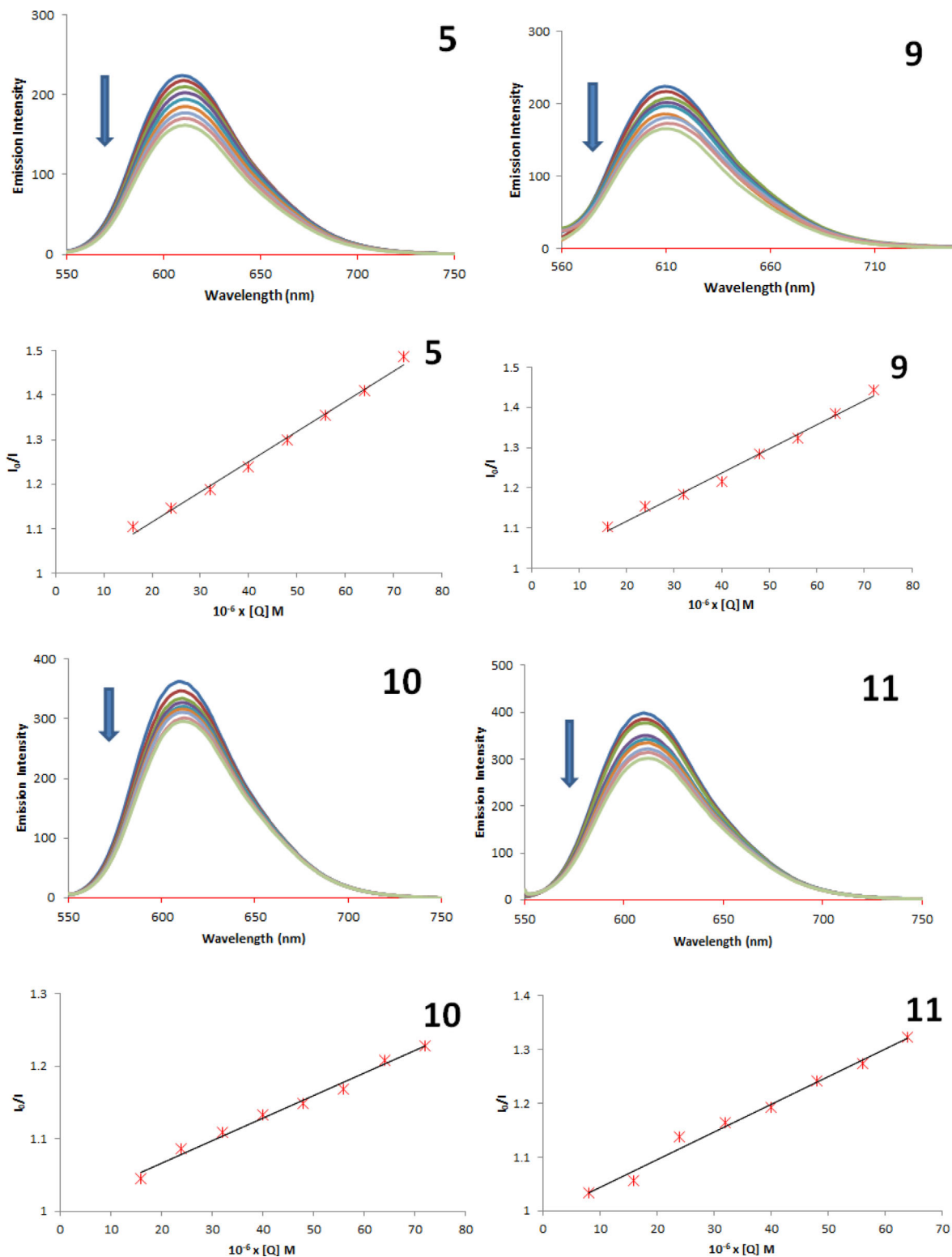


FIGURE 3 Top: Emission spectra of EB bound to DNA in the absence (red lines) and presence of compounds **5**, **9**–**11**. The red lines denote solutions: buffer + quencher. [EB] = 100 μ M, [DNA] = 100 μ M; [**5**], [**9**]–[**11**] = 0–100 μ M; pH = 7.4; λ_{ex} = 520 nm. The arrows show the emission intensity changes with increasing the concentrations of the quenchers. Bottom: Plots of I_0/I versus [Q]

(BSA). The fluorescence emission titration of BSA with selected compounds in the range of 300–500 nm was realized. It was observed that BSA exhibited a strong fluorescence emission band at 365 nm. The intensities of BSA reduced gradually with increasing

concentrations of **5**, **9**–**11**. Blue shift indicated that the fluorescence chromophore of serum albumin is placed in a more hydrophobic environment after the addition of selected compounds.^[32]

TABLE 3 The bimolecular quenching rate constant (k_q), Stern-Volmer constant (K_{sv}), and correlation coefficient (R) for the quenchers **5**, **9**–**11**

Quencher	k_q ($M^{-1} s^{-1}$)	K_{sv} (M_{-1})	R
5	$(6.3 \pm 0.2) \times 10^{11}$	$(6.3 \pm 0.2) \times 10^3$	0.9964
9	$(5.6 \pm 0.2) \times 10^{11}$	$(5.6 \pm 0.2) \times 10^3$	0.9944
10	$(3.1 \pm 0.2) \times 10^{11}$	$(3.1 \pm 0.2) \times 10^3$	0.9940
11	$(5.1 \pm 0.1) \times 10^{11}$	$(5.1 \pm 0.1) \times 10^3$	0.9935

The fluorescence quenching data were analyzed by using Equation 2^[33]:

$$\log[(I_0 - I)/I] = \log K_a + n \log [Q] \quad (2)$$

where I_0 and I are the emission intensities in the absence and presence of the quencher, K is the binding constant for **5**, **9**, **10**, or **11**-BSA interaction, n is the number of binding sites to BSA molecule, and $[Q]$ is the concentration of the quencher. The plots of $\log[(I_0 - I)/I]$ versus $\log[Q]$ are presented in Figure 4. The values of K_a and n are determined from the intercept and slope of the obtained straight lines. The binding parameters values for **5**, **9**–**11** BSA complexes are presented in Table 4. The values of n indicate that there is approximately one binding site in BSA for quinoxalinones during their interaction. The main factor in drugs availability to diffuse to target is the binding strength of the drug to BSA.^[34] When values of constants are in the range 10^4 – 10^6 than ligands bound reversibly to protein.^[35] Hence, K_a values show that binding between selected compounds and BSA is moderate. These values also showed that a reversible **5**, **9**, **10**-, or **11**-BSA complex is formed and **5**, **9**, **10**, or **11** can be stored and carried by BSA.

2.4 | Viscosity measurements

The DNA-viscosity is sensitive to the DNA-length changes in the presence of a DNA-binder.^[36] The values of relative specific viscosity $(\eta/\eta_0)^{1/3}$ relates to relative DNA-length (L/L_0) via Equation 3^[37,38]:

$$(\eta/\eta_0)^{1/3} = (L/L_0) \quad (3)$$

where η_0 and η are the specific viscosity contributions of DNA in the absence and in the presence of the ligands. In general, the DNA-viscosity enhances when the DNA-length increases as a result of separation distance of the DNA bases in order to host an intercalating compound. When intercalation is present, a planar ligand fragment is placed between adjacent base pairs, which induces lengthening of the helix.^[39–41] These interactions that result in the increase of the DNA length generate an increase of viscosity. On the other hand, non-classic intercalation (external interaction such as electrostatic interaction or groove-binding), does not lead to increase of the viscosity of the DNA solutions because the DNA-bases separation distance remains almost same. Moreover, as a result of such interaction a bend or kink of the DNA-helix may occur followed by a slight decrease of DNA-length and subsequently the DNA viscosity will be slightly affected or even decreased.^[42–44]

The values of relative specific viscosity $(\eta/\eta_0)^{1/3}$ versus R ($R = [\text{ligand}]/[\text{DNA}]$) in the absence and in the presence of complex in Tris-HCl buffer were plotted (Figure 5). Figure 5 shows that the addition of the ligands into a 0.01 mM DNA solution (up to $R = 1.0$) resulted in a significant increase of the relative viscosity of DNA sample. This increase was more pronounced upon addition of ligand **11**. On the basis of these results, we may deduce that the both ligands bind to the DNA in the mode of intercalation.^[45]

Li et al.^[46] showed that in presence of ethidium bromide, well known organic intercalator, the relative viscosity of DNA increased and the slope of the graph of $(\eta/\eta_0)^{1/3}$ versus R was 0.96. Consequently, we would expect that the relative viscosity of DNA increases with a slope between 0 and 0.96 if the intercalation of the ligands was either only one interaction mode or much stronger than other interaction(s). In our case, the relative viscosity of DNA increase with a slope of 0.97 (ligand **11**) and 0.789 (ligand **10**) (Figure 5) due to lengthening of the DNA helix as base pairs are separated to accommodate the aromatic chromophore of ligands. High value of the slope for ligand **11** corresponding to complexes of DNA with classical intercalating ligands. On the other hand, value of the slope for ligand **10** is slightly lower and it is reasonably believed that maybe other interactions between DNA and this ligand occurred, which leads to kinks or bends the DNA helix and reduces its effective length. Obtained results are in accordance with higher values of binding constant for this ligand, obtained from molecular docking, presented in next section.

2.5 | DNA and BSA docking

Molecular docking study with DNA dodecamer was performed to support the interactions and to find out the preferred binding modes of ligands (**5**, **9**–**11**) with DNA, as well reference compound, cisplatin. The best docked poses of the compounds with DNA dodecamer are displayed in Figure 6, and calculated results for binding energies and docked inhibition constant are summarized in Table 5. Docking analysis shows that all compounds interact with DNA through intercalation, which is in accordance with experimental results. As shown in Figure 6, the compounds comfortably fit in between the DNA nucleotides without rupturing the DNA double helix. The ligands **5** and **9** interact with DNA base pairs due to van der Waals and hydrophobic interactions as well as hydrogen bond with DT:B20. On the other hand, ligand **5**, more comfortably fits between DNA chains, due to smaller size, and intercalation is additionally stronger due to formation of hydrogen bond with DT:B20. The **11** ligand interacts with DNA base pairs through van der Waals interaction and hydrophobic interactions, and **10** ligand has additionally formation of two hydrogen bonds with DT:B19 and DG:A4. The existence of stronger interactions, primarily hydrogen bonds between oxygen atom from methoxy group of ligand **10** and guanine base in DNA molecule, and between $-\text{NH}$ from pyrazine ring of ligand **10** and thymine, is in accordance with results of viscosity measurements, due to lower values of the slope of ligand **10** compared to ligand **11** (Figure 5).

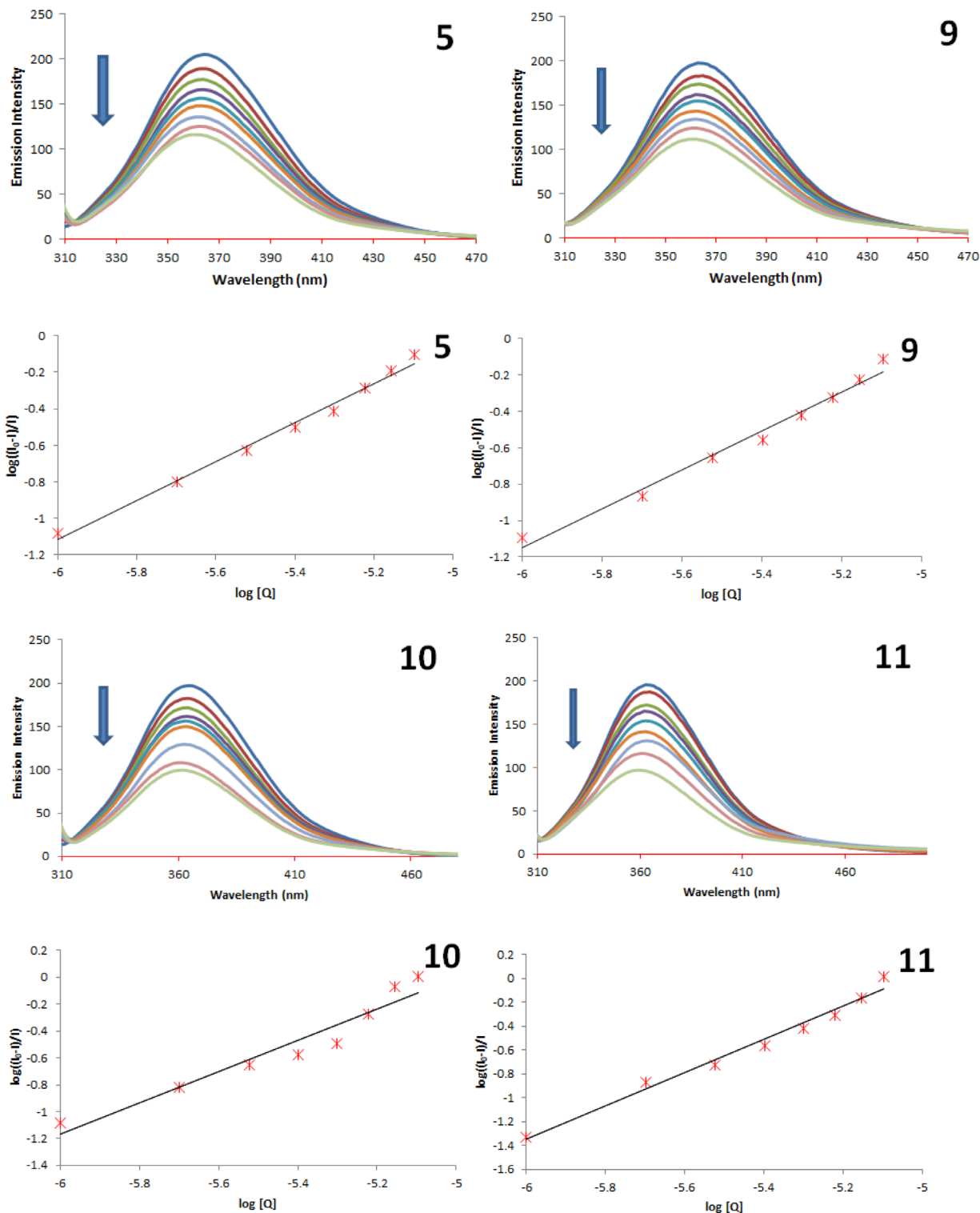


FIGURE 4 Top: Emission spectra of BSA in the absence (blue lines) and presence of compounds **5**, **9**–**11**. The red lines denote solutions: buffer + quencher. [BSA] = 10 μ M; [**5**], [**9**]–[**11**] = 0.0, 1.0, 2.0, 3.0, 4.0, 5.0, 6.0, 7.0, and 8.0; pH = 7.4; λ_{ex} = 280 nm

As can be seen from Table 5, **11** has higher negative value of free binding energy (ΔG) and has the highest binding affinity toward DNA compared to **10**. These results lead to conclusion that additional formation of H-bonds has a less influence on binding of ligands to DNA molecule comparing to geometrical fitting. It is also interesting to note that lowest value of free binding energy was obtained for ligand **5**,

probably due to smallest size which leads to most comfortable fit between DNA chains. Comparing results with cisplatin, similar values for ΔG are obtained for ligand **11**.

Molecular docking analysis of ligands with BSA were also conducted to validate the experimental results and to determine the possible binding modes and binding sites. The results of docking

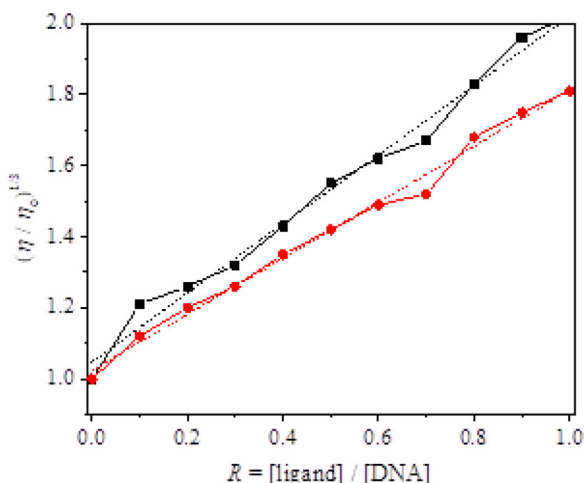
TABLE 4 Binding parameters (K_a and n) and the correlation coefficient (R) for interaction of **5**, **9**–**11** with BSA

Quencher	K_a (M)	n	R
5	$(1.9 \pm 0.1) \times 10^3$	1.06	0.9954
9	$(2.0 \pm 0.1) \times 10^3$	1.08	0.9908
10	$(1.1 \pm 0.1) \times 10^4$	1.16	0.9505
11	$(3.4 \pm 0.1) \times 10^4$	1.38	0.9906

studies of the compounds with BSA receptor are summarized in Table 5 and 3D binding environment are presented in Figure 7.

Analysis of results shows that all ligands interact with BSA in same binding pocket (Figure 7), located between two sub-domains IIa and IIIa, and this binding site is relatively exposed to solvent.^[47] The ligand **5** forms two H-bonds, one with Arg 185 and one with Tyr 160. The interaction between ligand **9** and BSA is stabilized due to hydrogen bond formation with Lys 136 and Thr 121. The interactions between **11** and the binding site of BSA occur through hydrogen bond formation between oxygen atoms from —C=O group of ligand and guanidinium group of Arg 185 and NH_2 group of Leu 115. Binding is additionally stronger because of π - π interactions between Lys 114 and aromatic ring of ligand. On the other hand, **10** forms two H-bonds with Leu 115, and one H-bond with Arg 185 and Lys 114, respectively.

Comparing all the results, it is obvious that for synthesized ligands **5**, **9**, and **10** the most important role in binding with BSA has Arg 185. Additionally, ligand **11** has lower values of ΔG than **10**, which indicates stronger binding affinity toward BSA, which is in accordance with results from fluorescence quenching. In comparison with results obtained for cisplatin docking, ΔG values for cisplatin were the lowest, probably due to less amount of H-bonds.

**FIGURE 5** Relative viscosity (η/η_0)^{1/3} of DNA (0.01 mM) in buffer solution (50 mM NaCl and 5 mM Tris-HCl at pH 7.4) in the presence of the ligands **10** (red circle) and **11** (black square) at increasing amounts (R). Dashed lines represent the fitted linear regression curve

2.6 | Assessment of anti- α -glucosidase activity

Evaluation of the inhibition of the α -glucosidase showed that two of the tested compounds expressed significant *in vitro* inhibition of the enzyme (Table 6). After absorbencies were read and blanks subtracted, the IC_{50} values of the compounds were calculated from dose response curves. Compound **11** showed the highest inhibition activity with IC_{50} value of $40.09 \pm 0.49 \mu\text{M}$, while compound **10** exhibited the lowest inhibition activity overall with IC_{50} $166.09 \pm 9.80 \mu\text{M}$. IC_{50} values for compounds **9**–**11** were less than IC_{50} values of standard antidiabetic drug (acarbose). These results are in concordance with some previous studies with quinoxalinones, that indicated that this type of scaffolds can inhibit α -glucosidase^[48] and have antidiabetic properties.^[49] The results suggest that compounds **10** and **11** could be further analyzed as new potential control postprandial hyperglycemia compounds.

2.7 | Assessment of anti-angiogenic effects

In order to assess the effect of the investigated compounds on *in vitro* angiogenesis, the tube formation assay was performed. As shown in Figure 8, EA.hy926 cells in the control aligned to form tube-like structures and crossing tubes with multicentric junctions. On the other hand, the treatment with sub-toxic IC_{20} dose of the investigated compounds of **5** ($45 \mu\text{M}$), **9** ($8 \mu\text{M}$), **10** ($5 \mu\text{M}$), and **11** ($9.5 \mu\text{M}$) resulted in a significant anti-angiogenic effect, which is reflected in the decrease in capillary tube formation. There is an apparent inhibition of the association of cells and formation of tubules and polygon structures. There are also literature data that show that benzoxazines and quinoxalinones are angiogenesis inhibitors.^[50,51]

3 | CONCLUSIONS

The cytotoxic activity of the compounds **1**–**20** against human cervix adenocarcinoma (HeLa), human colon carcinoma (LS174), non-small cell lung carcinoma (A549), and normal human fetal lung fibroblast cell line (MRC-5) was investigated. Compounds **5**, **9**–**11** showed a significant cytotoxic activity against all tested malignant cell lines. Based on these results, cell cycle distribution on HeLa cell line for **5**, **9**–**11** was evaluated. Compound **11** exerted the best effects, leading to a notable increase in G2/M phase in HeLa cells treated with both concentrations of the compound, which was coupled with a decrease in the percentage of cells in G1 phase. Values of quenching parameters for **5**, **9**–**11** indicate that these compounds have large affinity to substitute EB from the EB-DNA complex and bind strongly with DNA through intercalation that is in order with the constants obtained for potential metal-drugs. Molecular docking study with DNA dodecamer and BSA was performed to support the interactions and to find out the preferred binding modes of ligands (**5**, **9**–**11**) with DNA or BSA. Docking results shows that all compounds interact with DNA and BSA through intercalation, which is in accordance with experimental results. The results of the inhibition of the α -glucosidase suggest that compounds **10** and **11** could be further analyzed as new potential control postprandial hyperglycemia compounds.

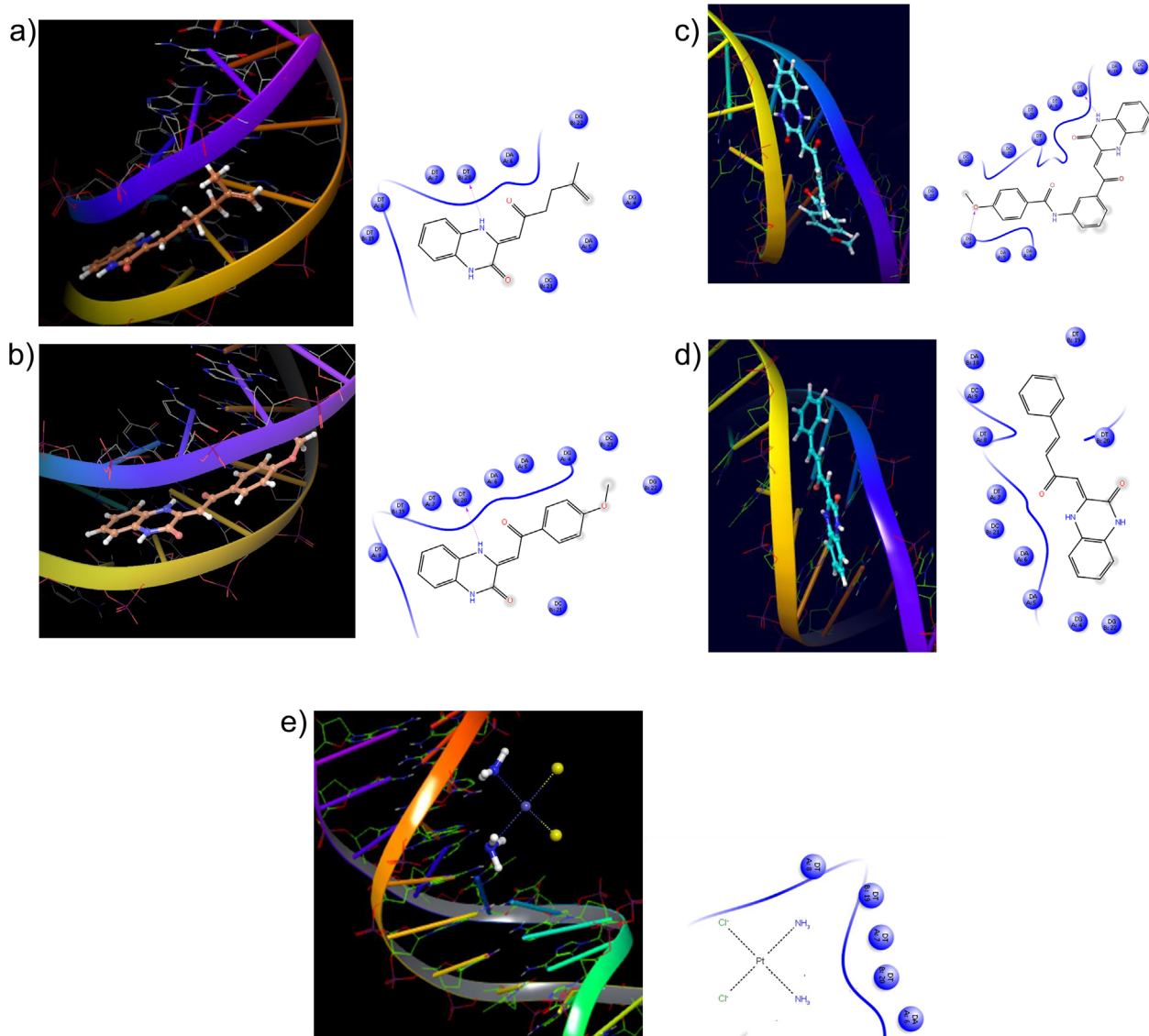


FIGURE 6 Docking results for DNA docking with ligands: (a) 5, (b) 9, (c) 10, (d) 11, and (e) cisplatin

TABLE 5 Docking parameters for 5, 9–11

Compound	Docking score	Free energy of binding (ΔG)/kJ/mol	Docked inhibition constant (K_i)/ μM
DNA			
5	-5.783	-39.17	0.137
9	-6.664	-46.09	0.008
10	-6.663	-33.16	1.553
11	-7.018	-37.11	0.315
Cisplatin	-6.345	-37.06	0.304
BSA			
5	-5.879	-31.43	3.114
9	-6.119	-33.63	1.282
10	-6.794	-21.73	155.986
11	-7.225	-28.11	11.894
Cisplatin	-5.321	-20.18	291.35

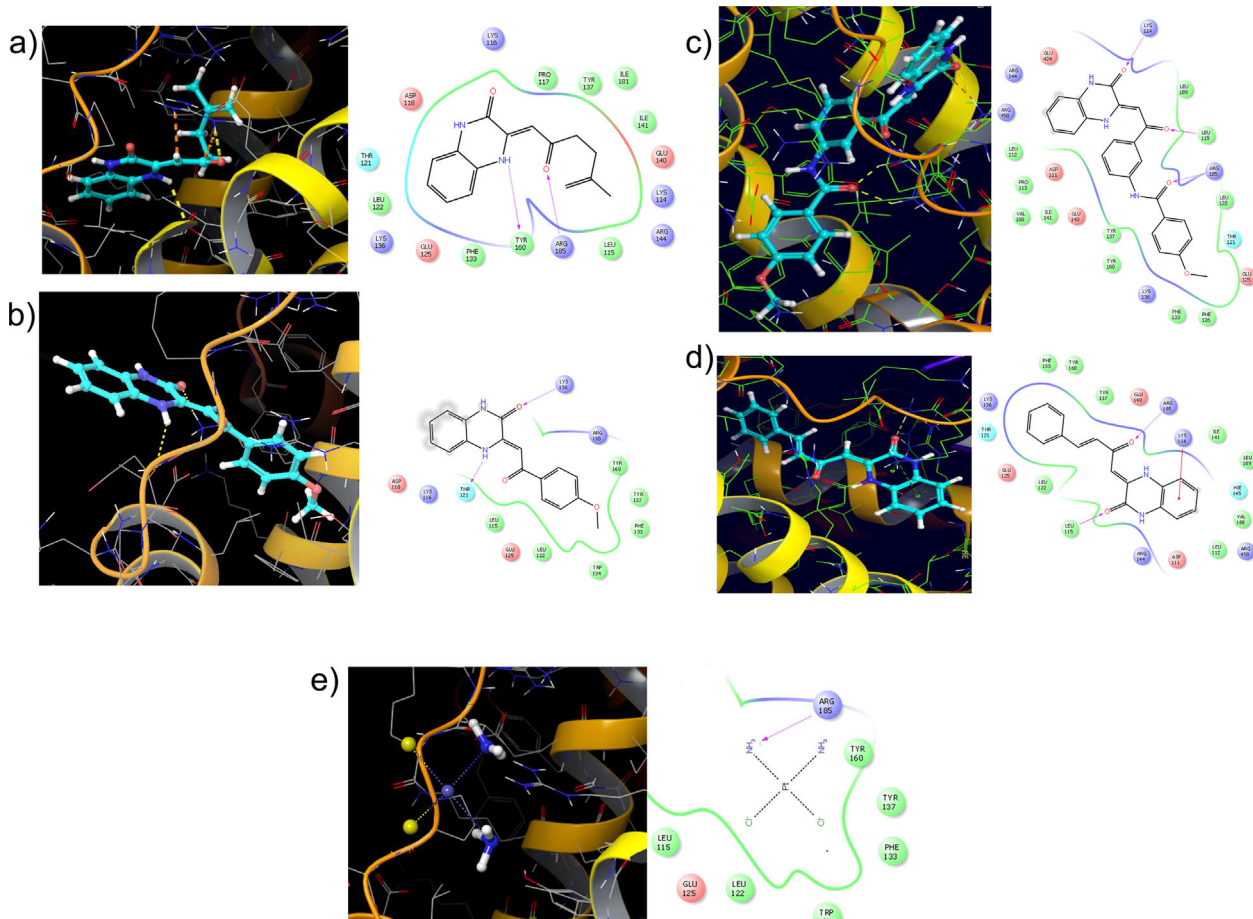


FIGURE 7 Docking results for BSA docking with ligands: (a) 5, (b) 9, (c) 10, (d) 11, and (e) cisplatin

4 | EXPERIMENTAL

4.1 | Biological activity

4.1.1 | Cell culture

Cervix adenocarcinoma cell line (HeLa), human colon carcinoma (LS174), non-small cell lung carcinoma (A549) and a normal cell line, human fetal lung fibroblast cell line (MRC-5) were grown in RPMI-1640 medium (Sigma) at 37°C. Media were supplemented with 10% fetal bovine serum, L-glutamine, and penicillin-streptomycin (Sigma).

TABLE 6 IC₅₀ ± SD values of anti-α-GIs activity of the investigated compounds 5, 9–11

Compounds	IC ₅₀ (μM)
5	166.09 ± 9.80
9	133.85 ± 8.05
10	52.54 ± 0.09
11	40.09 ± 0.49
Acarbose	145.43 ± 3.88

Results are expressed as mean ± standard deviation (SD).

4.1.2 | Treatment of cells

Stock solutions (10 mM) of the compounds, made in DMSO, were dissolved in a corresponding medium to the required working concentrations. Target cells HeLa (2000 cells per well), LS174 (7000 cells per well), A549 (5000 cells per well), and MRC-5 (5000 cells per well) were seeded into wells of a 96-well flat-bottomed microtiter plate. Twenty-four hours later, after the cell adherence, different concentrations of investigated compounds were added to the wells, except for the control cells to which only nutrient medium was added. Final concentrations reached in treated wells were in the range of 12.5–200 μM. The final concentration of DMSO solvent never exceeded 0.5%, which was non-toxic to the cells. All investigated concentrations were set up in triplicate. Nutrient medium with corresponding concentrations of investigated compounds, but without cells, was used as a blank, also in triplicate. The cultures were incubated for 72 h.

4.1.3 | Determination of IC₅₀ value

The effect of the investigated compounds on survival of the specified cell lines was determined by the microculture tetrazolium test (MTT) according to Mosmann^[52] with modification by Ohno and Abe^[53] 72 h

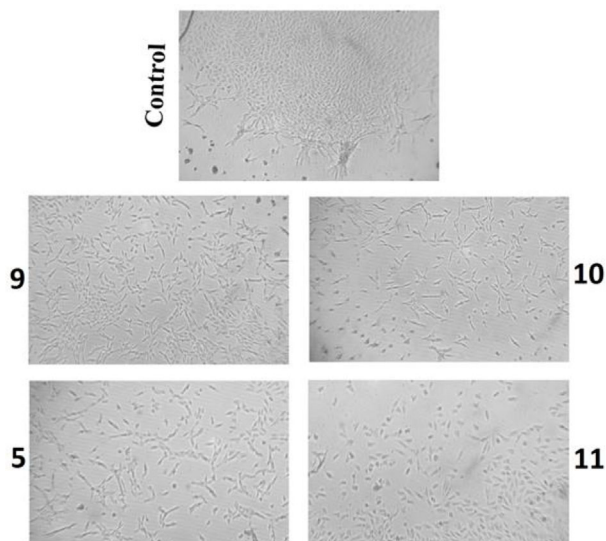


FIGURE 8 Effects of investigated compounds **5**, **9**, **10** and **11** on angiogenesis of endothelial cells. The IC_{20} values of these compounds on tube formation inhibition of EA.hy926 ranged from 5 to 45 μ M. Representative photomicrographs from one of three independent experiments

after addition of the compounds, as described earlier. Briefly, 20 mL of MTT solution (5 mg/mL phosphate-buffered saline) was added to each well. Samples were incubated for a further 4 h at 37°C in a humidified atmosphere of 95% air/5% CO₂ (v/v). Then 100 μ L of 100 g/L sodium dodecyl sulfate was added to dissolve the insoluble product formazan resulting from conversion of the MTT dye by viable cells. The absorbance (A) at 570 nm was measured 24 h later. The number of viable cells in each well was proportional to the intensity of the absorbance of light, which was read in an enzyme-linked immunosorbent assay (ELISA) plate reader. To determine cell survival (%), the A of a sample with cells grown in the presence of various concentrations of the investigated compounds was divided by the control optical density (the A of control cells grown only in nutrient medium) and multiplied by 100. In each experiment, the A of the blank was always subtracted from the A of the corresponding sample with target cells. IC_{50} is defined as the concentration of an agent inhibiting cell survival by 50% compared with a vehicle-treated control. All experiments were done in triplicate.

4.1.4 | Cell cycle analysis

Cervix adenocarcinoma (HeLa) cells, were seeded in six-well plates (3×10^5 cells/well), and after 24 h treated with investigated compounds, except control cells, and incubated at 37°C for the next 24 h. Concentrations used corresponded to IC_{50} and $2 \times IC_{50}$ values. After the incubation, the cells were collected by trypsinization, and fixed in ice-cold 70% ethanol for 1 h on ice, then at -20°C for at least a week. After fixation, the cells were washed in PBS and pellets obtained by centrifugation were treated with RNase (100 μ g/mL) at 37°C temperature for 30 min and then

incubated with propidium iodide (PI) (40 μ g/mL) for at least 30 min. DNA content and cell-cycle distribution were analyzed using a Becton Dickinson FACSCalibur flow cytometer. Flow cytometry analysis was performed using CellQuestR (Becton Dickinson, San Jose, CA, USA) software on a minimum of 10000 cells per sample.^[54]

4.1.5 | Tube formation assay

Twenty-four well plates were coated with 200 μ L of Corning® Matrigel® basement membrane matrix (Corning: cat. number 356234). Plates were incubated for 2 h. After that, suspensions of EA.hy926 cells were added into plates. In control cell sample complete nutrient medium was added, while solutions of sub-toxic concentrations (IC_{20}) of extracts with nutrient medium were added to other samples. Those concentrations were obtained by MTT test after 24 h treatment of EA.hy926 cells with investigated extracts. The 24 h incubation in the assay was at 37°C in an atmosphere of 5% CO₂ and humidified air. After incubation, photomicrographs of target cells were captured under the inverted phase-contrast microscope.^[55]

4.1.6 | α -Glucosidase inhibitory activity

The α -glucosidase inhibitory activity was estimated by the modification of the procedure described by McCue et al.^[56] with some modification. The enzyme solution was set at 400 mU/mL of α -glucosidase (Sigma-Aldrich) in a 0.1 mol phosphate buffer (pH = 6.7). For each well, we used 50 μ L of the tested extract in DMSO, diluted in a 0.1 mol phosphate buffer (pH = 6.7) so that the final concentrations of the extracts in each well were 166.67, 83.33, 41.67, 20.83, 10.42, 5.21 μ g/mL. In 96-well plates, we preincubated 50 μ L of extract dilutions with 50 μ L of enzyme solution for each well at 37°C for 15 min. The reaction was started by adding 50 μ L of substrate solution (1.5 mg/mL PNP-G (*p*-nitrophenyl α -D-glucopyranoside, Sigma-Aldrich) in the buffer), and after measuring absorbance A1 at 405 nm, the solution was incubated at 37°C for 15 min. Then second absorbance A2 was measured at 405 nm. Acarbose (Sigma-Aldrich) was used as a positive control. Percent of the enzyme inhibition was calculated as $100 \times (A2S - A1S)/(A2B - A1B)$, where A1B, A2B and A1S, A2S represent the absorbance of the blank (phosphate buffer, DMSO, enzyme dilution, and PNP-G dilution) and the sample, respectively. All tests were done in duplicate.

Calf-thymus DNA (CT-DNA), BSA (bovine serum albumin), ethidium bromide (EB), and [3-(4,5-dimethylthiazol-2-yl)-2,5-diphenyltetrazolium bromide (MTT)] were purchased from Sigma. Phosphate buffered saline (PBS) tablets were purchased from Fisher BioReagents. A solution of CT-DNA and EB in distilled water was prepared in 10 mM PBS buffer (pH = 7.4). A solution of CT-DNA in the above buffer with a ratio of about 1.8–1.9:1 corresponding to the absorbance at 260–280 nm, indicating the sufficient protein free nature of DNA. Concentration of CT-DNA was measured at 260 nm by UV absorbance.

4.2 | Fluorescence experiments for a protein binding study

BSA solution (200 μM) was prepared in 10 mM PBS buffer at pH = 7.4 and stored in the dark at 4°C for 3 days. The 5, 9–11-BSA complexes were prepared by independently incubating a constant amount of BSA with increasing amounts of tested compounds. The molar ratios of BSA: quenchers (5, 9, 10, or 11) followed the order: 1:0 (control), 1:0.1, 1:0.2, 1:0.3, 1:0.4, 1:0.5, 1:0.6, 1:0.7, 1:0.8, in a total volume of 5.0 mL, pH = 7.4, at 25°C. The quencher-BSA solutions were incubated for 3 h and the absorption spectra were recorded in the range of 300–450 nm and the maximal fluorescence intensities were used to calculate quenching parameters.

4.3 | Fluorescence experiments for a DNA binding study

All the DNA binding experiments were carried out in 10 mM PBS buffer at pH = 7.4. The absorption titration with CT-DNA was by keeping the concentration of the DNA constant while varying the concentrations of tested compounds. The solution of 5, 9–11-DNA were incubated 24 h before the spectra were recorded. The fluorescence intensities were measured with the excitation wavelength set at 527 nm and the fluorescence emission at 610 nm.

4.4 | Viscosity measurements

The viscosity of a DNA solution was measured in the presence of increasing amounts of complexes using Ubbelohde viscosimeter (SI Analytics GmbH, Mainz, Germany, type no. 525 03) by measuring the flow rate of the liquid. Viscosimeter was filled with experimental liquid and placed vertically in glass sided thermostat maintained constant to ± 0.01 K, with standard uncertainty of controlled temperature of ± 0.02 K. After thermal equilibrium is attained, the flow time of liquids was recorded with a digital stopwatch with an accuracy of ± 0.001 s. All measurements were performed at 310.15 K. Results were obtained as the mean value of at least 10 viscosity measurements and data were presented as $(\eta/\eta_0)^{1/3}$ against R , where η is the viscosity of DNA in the presence of ligand, η_0 is the viscosity of DNA alone in the buffer solution, and R is mole ratio of ligands/DNA. The DNA concentration was fixed at $1 \cdot 10^{-5}$ mol/dm³. The viscosity values were calculated from the observed flow time of the DNA-containing solutions (t) corrected for the flow time of the buffer alone (t_0), $\eta = (t - t_0)/t_0$. Relative standard uncertainty of determining the viscosity with Ubbelohde viscosimeter was found to be less than 1%.

4.5 | Computational method

For DNA docking study structure of B-DNA dodecamer was extracted from the crystal structure (pdb: 1BNA) and for bovine serum albumine (BSA) crystal structure with pdb 3VO3 was used. The structures were processed with the Protein Preparation Wizard in the Schrödinger 2015-02 suite package.^[57] The structures integrity was checked and adjusted, and missing residues and loop were added using Prime.^[58,59]

Hydrogen atoms were added after deleting any original ones, followed by adjustment of bond orders for residues and the ligands. The protonation and tautomeric states of residues were adjusted to match a pH of 7. Active site water molecules beyond 5.0 Å from the ligand were deleted. Hydrogen bond sampling with adjustment of active site water molecule orientations was performed using PROPKA at pH 7.^[60] Then, the enzyme was subjected to geometry refinement using an OPLS-2005^[61] force field restrained minimization with convergence of heavy atoms to an RMSD of 0.3 Å.

All ligand structures have been firstly geometrically optimized employing empirically dispersion-corrected B3LYP exchange-correlation functional (B3LYP-D3) with 6-31 + G(d,p) basis set using Macro Model/Conformational Search and adequately prepared for further docking using LigPrep with force field OPLS-2005.^[62]

The receptor grid for each target was prepared using the OPLS-2005 force field, and docking was performed using Glide with standard precision.^[63] Flexible ligand sampling was considered in the docking procedure. All poses were subjected to post-docking minimization. The best-docked structures for each ligand were determined, based on the model energy score which combines the energy grid score, the binding affinity, the internal strain energy and the Coulomb-van der Waals interaction energy scores.

ACKNOWLEDGMENT

The authors are grateful to the Ministry of Education, Science and Technological Development of the Republic of Serbia for financial support (Grants 172011 and 175011).

CONFLICT OF INTEREST

The authors have declared no conflicts of interest.

ORCID

Nenad Janković  <http://orcid.org/0000-0002-2295-9410>

REFERENCES

- [1] Y. Ramli, A. Moussaif, K. Karrouchi, E. M. Essassi, *J. Chem.* **2014**, 2014 (ID 563406).
- [2] J. A. Pereira, A. M. Pessoa, M. N. Cordeiro, R. Fernandes, C. Prudêncio, J. P. Noronha, M. Vieira, *Eur. J. Med. Chem.* **2015**, 97, 664.
- [3] T. J. Sindhu, S. D. Arikatt, G. Vincent, M. Chandran, A. R. Bhat, K. Krishnakumar, *Inter. J. Pharm. Sci. Res.* **2013**, 4, 134.
- [4] D. P. Singh, S. K. Deivedi, S. R. Hashim, R. G. Singhal, *Pharmaceuticals* **2010**, 3, 2416.
- [5] S. Noorulla, N. Sreenivasulu, *Inter. J. Pharm. Sci. Res.* **2011**, 2, 2337.
- [6] Y. Yang, S. Zhang, B. Wu, M. Ma, X. Chen, X. Qin, M. He, S. Hussain, C. Jing, B. Ma, C. Zhu, *ChemMedChem* **2012**, 7, 823.
- [7] J. Balzarini, E. De Clercq, A. Carbonez, V. Burt, J.-P. Kleim, *AIDS Res. Hum. Retroviruses* **2000**, 16, 517.
- [8] P. Sanna, A. Carta, M. Loriga, S. Zanettiand, L. Sechi, *Farmaco* **1999**, 54, 161.

- [9] A. Carta, M. Loriga, S. Prisas, G. Paglietti, P. La Colla, B. Busonera, G. Collu, R. Loddo, *Med. Chem.* **2006**, *2*, 113.
- [10] B. Zarranz, A. Jaso, I. Aldana, A. Monge, *Bioorg. Med. Chem.* **2003**, *11*, 2149.
- [11] B. Lippert, *Cisplatin: Chemistry and Biochemistry of a Leading Anticancer Drug*. Wiley-VCH, Interscience, **1999**.
- [12] M. Arsenijević, M. Milovanović, V. Volarević, D. Canović, N. Arsenijević, T. Soldatović, S. Jovanović, Z. D. Bugarčić, *Trans. Met. Chem.* **2012**, *37*, 481.
- [13] F. P. T. Hamers, W. H. Gispen, J. P. Neijt, *Eur. J. Cancer* **1991**, *3*, 372.
- [14] R. W. Schrier, *J. Clin. Invest.* **2002**, *110*, 743.
- [15] I. Arany, R. L. Safirstein, *Semin. Nephrol.* **2003**, *23*, 460.
- [16] I. Ott, R. Gust, *Arch. Pharm.* **2007**, *340*, 117.
- [17] J. Petronijević, Z. Bugarčić, G. A. Bogdanović, S. Stefanović, N. Janković, *Green Chem.* **2017**, *19*, 707.
- [18] K. Zhang, W. Liu, *Int. J. Electrochem. Sci.* **2011**, *6*, 1669.
- [19] C. Bertucci, E. Domenici, *Curr. Med. Chem.* **2002**, *9*, 1463.
- [20] S. F. Sun, B. Zhou, H. N. Hou, Y. Liu, G. Y. Xiang, *Int. J. Biol. Macromol.* **2006**, *39*, 197.
- [21] P. B. Kandagal, S. Ashoka, J. Seetharamappa, S. Shaikh, Y. Jadegoud, O. B. Ijare, *J. Pharm. Biomed. Anal.* **2006**, *41*, 393.
- [22] S. M. Weis, D. A. Cheresch, *Nat. Med.* **2011**, *17*, 1359.
- [23] P. Carmeliet, R. K. Jain, *Nature* **2011**, *473*, 298.
- [24] M. Kowanetz, N. Ferrara, *Clin. Cancer Res.* **2006**, *12*, 5018.
- [25] S.-G. Cho, Z. Yi, X. Pang, T. Yi, Y. Wang, J. Luo, Z. Wu, D. Li, M. Liu, *Cancer Res.* **2009**, *69*, 7062.
- [26] H. Xin, A. Herrmann, K. Reckamp, W. Zhang, S. Pal, M. Hedvat, C. Chang, W. Liang, A. Scuto, S. Weng, D. Morosini, Z. A. Cao, M. Zinda, R. Figlin, D. Huszar, R. Jove, H. Yu, *Cancer Res.* **2011**, *71*, 6601.
- [27] R. I. Geran, N. H. Greenberg, M. M. Macdonald, A. M. Schumacher, B. J. Abbou, *Cancer Chemoth. Rep.* **1972**, *3*, 1.
- [28] B. C. Baguley, M. LeBret, *Biochemistry* **1994**, *23*, 937.
- [29] R. Lakowicz, G. Weber, *Biochemistry* **1973**, *12*, 4161.
- [30] E. Sundaravadeivel, S. Vedavalli, M. Kandaswamy, B. Vargheseb, P. Madankumar, *RSC Adv.* **2014**, *4*, 40763.
- [31] N. Joksimović, D. Baskić, S. Popović, M. Zarić, M. Kosanić, B. Ranković, T. Stanojković, S. B. Novaković, G. Davidović, Z. Bugarčić, N. Janković, *Dalton Trans.* **2016**, *45*, 15067.
- [32] V. D. Suryawanshi, L. S. Walekar, A. H. Gore, P. V. Anbhule, G. B. Kolekar, *J. Pharm. Anal.* **2016**, *6*, 56.
- [33] W. L. Gabler, *Res. Commun. Chem. Pathol. Pharmacol.* **1991**, *72*, 39.
- [34] G. Colmenajero, A. Alvarez-Pedraglio, J. L. Lavandera, *J. Med. Chem.* **2001**, *44*, 4370.
- [35] T. Topala, A. Bodoki, L. Oprean, R. Oprean, *Clujul Med.* **2014**, *87*, 215.
- [36] D. S. Sigma, A. Mazuder, D. M. Pemn, *Chem. Rev.* **1993**, *93*, 2295.
- [37] D. Li, J. Tian, W. Gu, X. Liu, S. Yan, *J. Inorg. Biochem.* **2010**, *104*, 171.
- [38] J. L. Garcia-Gimenez, M. Gonzalez-Alvarez, M. Liu-Gonzalez, B. Macias, J. Borrás, G. Alzuet, *J. Inorg. Biochem.* **2009**, *105*, 923.
- [39] A. Tarushi, E. Polatoglou, J. Kljun, I. Turel, G. Psomas, D. P. Kessissoglou, *Dalton Trans.* **2011**, *40*, 9461.
- [40] K. C. Skyrianou, C. P. Raptopoulou, V. Psycharis, D. P. Kessissoglou, G. Psomas, *Polyhedron* **2009**, *28*, 3265.
- [41] K. C. Skyrianou, E. K. Efthimiadou, V. Psycharis, A. Terzis, D. P. Kessissoglou, G. Psomas, *J. Inorg. Biochem.* **2009**, *103*, 1617.
- [42] C. Tolia, A. N. Papadopoulos, C. P. Raptopoulou, V. Psycharis, C. Garino, L. Salassa, G. Psomas, *Inorg. Biochem.* **2013**, *123*, 53.
- [43] A. Tarushi, C. P. Raptopoulou, V. Psycharis, D. P. Kessissoglou, A. N. Papadopoulos, G. Psomas, *Inorg. Biochem.* **2014**, *140*, 185.
- [44] A. Tarushi, S. Perontsis, A. G. Hatzidimitriou, A. N. Papadopoulos, D. P. Kessissoglou, G. Psomas, *J. Inorg. Biochem.* **2015**, *149*, 68.
- [45] G. Cohen, H. Eisenberg, *Biopolymers* **1969**, *8*, 45.
- [46] F. H. Li, G. H. Zhao, H. X. Wu, H. Lin, X. X. Wu, S. R. Zhu, H. K. Lin, J. *Inorg. Biochem.* **2006**, *100*, 36.
- [47] B. Bhattacharya, S. Nakka, L. Guruprasad, A. Samanta, *J. Phys. Chem. B* **2009**, *113*, 2143.
- [48] F. A. S. Alasmary, F. S. Alnahdi, A. Ben Bacha, A. M. El-Araby, N. Moubayed, A. M. Alafeefy, A. M. El-Araby, *J. Enzyme. Inhib. Med. Chem.* **2017**, *32*, 1143.
- [49] N. V. Kulkarni, V. K. Revankar, B. N. Kirasur, M. H. Hugar, *Med. Chem. Res.* **2012**, *21*, 663.
- [50] S. Al-Rawi, T. Meehan-Andrews, C. Bradley, J. Al-Rawi, *Invest. New Drugs* **2015**, *33*, 45.
- [51] L. Shi, J. Zhou, J. Wu, J. Cao, Y. Shen, H. Zhou, X. Li, *Bioorg. Med. Chem.* **2016**, *24*, 1840.
- [52] T. Mosmann, *J. Immunol. Methods* **1983**, *65*, 55.
- [53] M. Ohno, T. Abe, *J. Immunol. Methods* **1991**, *145*, 199.
- [54] R. H. Clothier, *Methods Mol. Biol.* **1995**, *43*, 109.
- [55] E. Aranda, G. I. Owen, *Biol. Res.* **2009**, *42*, 377.
- [56] P. McCue, Y. I. Kwon, K. Shetty, *J. Food Biochem.* **2005**, *29*, 278.
- [57] Schrödinger Suite Prote in Preparation Wizard. Schrödinger, LLC; New York, NY, **2015**.
- [58] M. P. Jacobson, R. A. Friesner, Z. Xiang, B. Honig, *J. Mol. Biol.* **2002**, *320*, 597.
- [59] Schrödinger Suite, Prime, Schrödinger, LLC; New York, NY, **2015**.
- [60] M. Rostkowski, M. Olsson, C. Sondergaard, J. Jensen, *BMC Struct. Bio.* **2011**, *11*, 1.
- [61] W. L. Jorgensen, J. Tirado-Rives, *Proc. Natl. Acad. Sci. USA* **2005**, *102*, 6665.
- [62] Schrödinger Suite, LigPrep, Schrödinger, LLC; New York, NY, **2015**.
- [63] Schrödinger Suite, Glide, Schrödinger, LLC; New York, NY, **2012**.

SUPPORTING INFORMATION

Additional Supporting Information may be found online in the supporting information tab for this article.

How to cite this article: Petronijević J, Janković N, Stanojković TP, et al. Biological evaluation of selected 3,4-dihydro-2(1H)-quinoxalinones and 3,4-dihydro-1,4-benzoxazin-2-ones: Molecular docking study. *Arch Pharm Chem Life Sci.* 2018;1-13.
<https://doi.org/10.1002/ardp.201700308>